Jets and the hadronic final state at HERA

T. Schörner-Sadenius[a] on behalf of the H1 and ZEUS collaborations

[a]Universität Hamburg, IExpPh, Luruper Chaussee 149, 22761 Hamburg, Germany

Recent results on jets and the hadronic final state from the HERA collaborations H1 and ZEUS are reviewed.

1. INTRODUCTION

Until the year 2000, the HERA experiments H1 and ZEUS have collected integrated luminosities of about 130 pb^{-1}. A large number of interesting results on jets and the hadronic final state from this 'HERA 1' data taking period have already been published, and many more analyses are still ongoing.

In 2001/2002 the HERA machine and also the experiments have undergone major changes with the aim of increasing the delivered luminosity by a factor of five. Due to technical problems, efficient data taking could not start before the end of 2003. Therefore, new results from the 'HERA 2' data taking period are only now starting to come out.

In the recent years the analysis work on the HERA 1 data has concentrated on making optimal use of the high statistics and either decreasing statistical (and also systematic) errors or performing more and more differential measurements. In addition, increased statistics allows for the discovery or first measurement of new or exotic phenomena.

This contribution will highlight new results concerning jets and the hadronic final state at HERA which were published or made preliminary since the EPS03 conference in Aachen.

2. EVENT SHAPE VARIABLES

Event shape variables like the thrust T, broadening B or the C parameter measure aspects of the topology of an event's hadronic final state. These variables are inclusive and infrared safe so that hadronisation corrections can be estimated using power correction (PC) models.

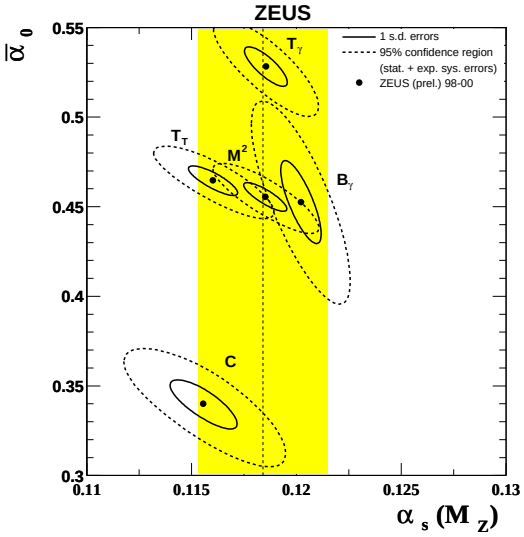

Figure 1. ZEUS event shape variables: Simultaneous fit of α_S and the PC parameter $\overline{\alpha_0}$ to the mean of event shape variables using NLO+PC predictions.

ZEUS has performed measurements of event shape variables in the Breit frame in the range $80 < Q^2 < 20480$ GeV^2 [1]. The choice of the Breit frame assures that the current region, i.e. the direction of flight of the scattered parton, resembles a single hemisphere in e^+e^- collisions, thus making the HERA results comparable to results from other colliders, especially LEP.

The PC model suggests that non-perturbative corrections to the predictions of observables can be parametrised with a universal parameter $\overline{\alpha_0}$

according to $\langle F\rangle = \langle F\rangle_{NLO} + \langle F\rangle_{pow}(\alpha_S, \overline{\alpha_0})$. So if the next-to-leading (NLO) prediction $\langle F\rangle_{NLO}$ exists, one can fit for α_S and for the universal parameter $\overline{\alpha_0}$.

In addition to the power corrections, next-to-leading log (NLL) resummations can help to improve the description of differential event shape distributions. The use of NLL sums requires a matching with the NLO prediction in order to avoid double-counting of terms.

Fitting the means of the event shape variables with NLO+PC predictions one obtains the results for α_S and $\overline{\alpha_0}$ shown in Figure 1. The resulting α_S values are consistent with the current world average, $\alpha_S = 0.118$. The data suggest $\overline{\alpha_0} = 0.5$ consistently for all event shape variables except for the C parameter, the fit of which is extremely sensitive to the fit range in the ZEUS analysis (in contrast to H1 measurements). This result for $\overline{\alpha_0}$ is roughly compatible with the results from other experiments.

3. PROMPT PHOTON PRODUCTION

The ZEUS collaboration has for the first time measured prompt photon production in DIS in the full HERA 1 data sample of about 120 pb^{-1} [2]. Prompt photons are required to be well-isolated and are identified using calorimeter cluster shape information; neutral particle backgrounds are subtracted using Monte Carlo (MC) predictions.

Two analyses were applied to the data: In the first, inclusive prompt photon production is studied, and the data are compared to the leading-order (LO) MC models HERWIG and PYTHIA; none of the models is able to describe all features of the data, and both are far away from the data in terms of normalisation.

In the second analysis, a jet in the central rapidity region was required in addition to the isolated photon. Jets were reconstructed using a cone algorithm in the laboratory frame; their transverse energy had to be in excess of 6 GeV, and their pseudo-rapidity between -1.5 and 1.8. The measurements, which yield a total cross-section of 0.86 pb for prompt photon plus jets, are again compared to HERWIG and PYTHIA,

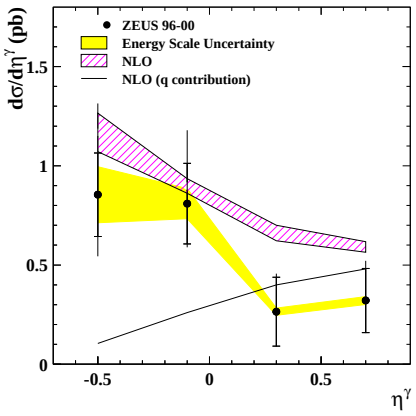

Figure 2. ZEUS prompt photon plus jet sample: photon pseudo-rapidity distribution. The data, which are shown together with the energy scale uncertainty band, are compared to the NLO calculations for which the renormalisation scale uncertainty is also indicated. Also shown is the contribution to the cross-section which is due to prompt photon emission from the quark line.

but there exists also an NLO QCD calculation for this signature. PYTHIA and HERWIG manage to describe the shapes of the photon and jet transverse energy distributions, but they fail in describing both pseudo-rapidity distributions. In addition, their normalisation is again of by factors of about 2 (4) for PYTHIA (HERWIG).

The NLO QCD calculation for the prompt photon plus jet analysis predicts a cross-section of about 1.33 pb, which is supposed to be lowered by hadronisation corrections by about 30-40 %. The normalisation of the calculation is therefore compatible with the data. As an example, Figure 2 shows the prompt photon pseudo-rapidity distribution. The data are in agreement with the NLO predictions; however, the statistical uncertainty of the measurement is very large. The same is true for the jet transverse energy distribution. However, the calculations predict a too large cross-section at low photon transverse energies and at high (forward) jet pseudo-rapidities.

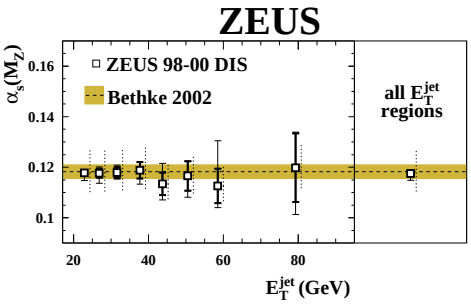

Figure 3. ZEUS α_S measurements based on the mean integrated jet shape $\langle\psi(r = 0.5)\rangle$ in DIS events as a function of the jet transverse energy. The data are shown together with the combined α_S value and the world average.

4. NEWS FROM JET PHYSICS

4.1. Determinations of α_s from jet shapes

The ZEUS collaboration has measured the substructure dependence of jet cross-sections in photoproduction and DIS with the aim of extracting the strong coupling parameter α_S [3]. ZEUS used mainly the mean integrated jet shape $\langle\psi(r)\rangle$ which is defined as:

$$\langle\psi(r)\rangle = \frac{1}{N_{jets}}\Sigma_{jets}\frac{E_T(r)}{E_T^{jet}}. \quad (1)$$

Here, N_{jets} is the total number of jets in the sample, $E_T(r)$ is the transverse energy within a cone of radius r around the jet axis, and E_T^{jet} is the transverse energy of the jet. The jet shape was measured, for example, as a function of the jet transverse energy in DIS events. For each data point, an α_S value is determined (Figure 3); the resulting values are evolved to the mass of the Z, and the different values are combined into one $\alpha_S(M_Z)$ value: $\alpha_S = 0.1176\pm^{0.0091}_{0.0072}$, where only the dominating theoretical uncertainty is given.

4.2. Summary on α_S

Figure 4 gives an overview of various α_S measurements performed by the HERA collaborations in jet events. The measurements are in perfect agreement with the world average; the already very good precision of the measurements, which has been increased over the past few years, will be even more increased once the HERA 2 data are collected and analysed.

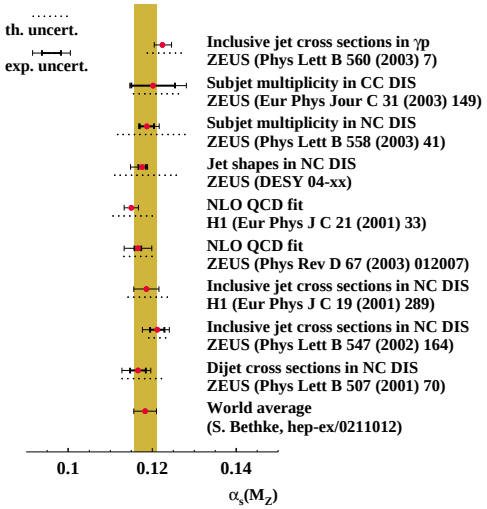

Figure 4. A summary of α_S measurements from H1 and ZEUS jet analyses.

4.3. Jets in global QCD fits

Jet data from the HERA experiments can be used for more than just determinations of the strong coupling. Recently, the ZEUS collaboration has started to include jet data into their global QCD fits [4], thus supplementing the usual F_2 data. The aim of using jet data is to improve the precision of the PDF measurements, especially the gluon, at high values of x.

The use of jet data in the fits, however, requires a fast evaluation of the NLO predictions for the jet cross-sections. During the minimisation procedure, this prediction has to be performed many thousand times. The usual typical 8 hours for sufficient statistics clearly is not acceptable here. The way around this problem is based on the following method. The jet cross-section can be written as the convolution of the hard partonic cross-section $\hat{\sigma}$ with the PDF f_a:

$$\sigma = \Sigma_a\Sigma_{n=1}^{\infty}\alpha_S^n \int d\eta f_a(\eta,\mu_F)\cdot\hat{\sigma}_n(\eta,\mu_F) \quad (2)$$

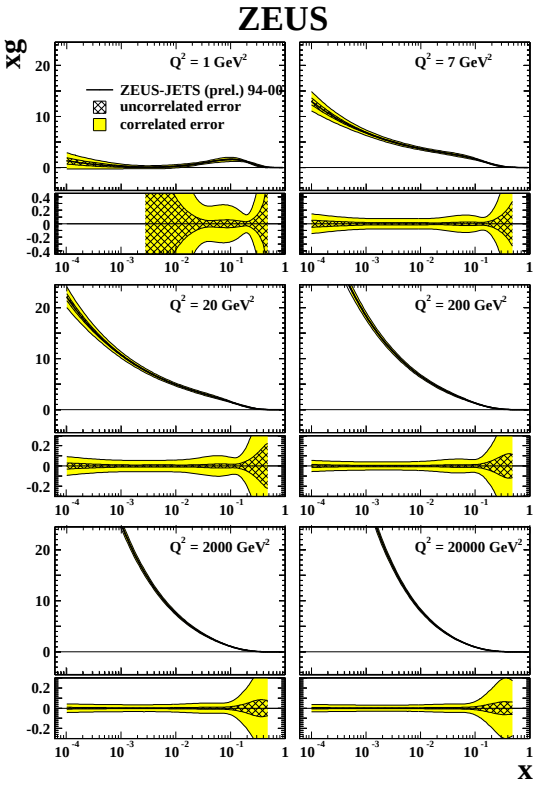

Figure 5. ZEUS global QCD fit. The gluon density as a function of x is shown for various Q^2 bins. Presented are the results of the ZEUS fit including jet data.

Here, the first sum runs over all parton flavours. Defining a sufficiently finely binned grid in (η, μ_F) and assuming that the PDF $f_a(\eta, \mu_F)$ is flat in every bin separately, one can write the cross-section in one bin of the (η, μ_F) grid as:

$$\sigma(\eta, \mu_F) \sim \Sigma_a f_a(\eta, \mu_F) \cdot \Sigma_{n=0}^{\infty} \alpha_S^n \int d\eta \hat{\sigma}_n(\eta, \mu_F) \quad (3)$$

where the integration is now only over the corresponding bin in η. The summation of all pieces $\sigma(\eta, \mu_F)$ leads again to the total cross-section. The benefit of this method is that the coefficients (the integrals in Equation 3) have to be evaluated only once since they are independent of the PDFs; they can thus be stored in a grid and be convoluted with any PDF provided from the outside, for example from the fitting program. The convolution then takes only parts of a second, which allows for the use of this cross-section evaluation in fitting programs.

The effect of the use of jet data can be viewed in Figure 5 which shows the results for the gluon density as achieved by the ZEUS fit using inclusive (F_2) and jet data. The data are shown as function of x in different bins of Q^2. A clear decrease of the size of the uncertainty for the low-Q^2 region is found; the effect is less striking for higher Q^2 values.

For the future, ZEUS aims at including further jet data from photoproduction, heavy flavour production and also, if possible, from proton-antiproton collisions into the QCD fit.

4.4. FROM PHOTOPRODUCTION TO DIS

The transition region from photoproduction to DIS has since long been problematic in the theoretical description. The HERA collaborations have published new results on this topic [5,6,7].

H1 has analysed dijet cross-sections in the kinematic region $5 < Q^2 < 100$ GeV^2 [5]. The data, taken in the years 1996 and 1997, are compared to direct NLO calculations. Overall good agreement between data and predictions is observed. However, comparing the data to NLO predictions for dijet events with small azimuthal separation between the two hardest jets shows a clear excess of the data over the prediction. This discrepancy can be cured partly using a NLO three-jet calculation; however discrepancies remain at low Q^2 and x.

Figure 6 shows the ZEUS dijet cross-section as a function of Q^2 over a wide kinematic range from 0 GeV^2 to 2000 GeV^2 [6]. The data are separated into regions of direct- and resolved-enriched events by means of the observable x_γ which quantifies the fraction of the photon's energy that entered the hard scattering. Shown is also the NLO QCD prediction. For the DIS regime, the NLO calculation, which does not include resolved contributions, clearly fails to describe the low-x_γ component (independent of Q^2) and also the low-

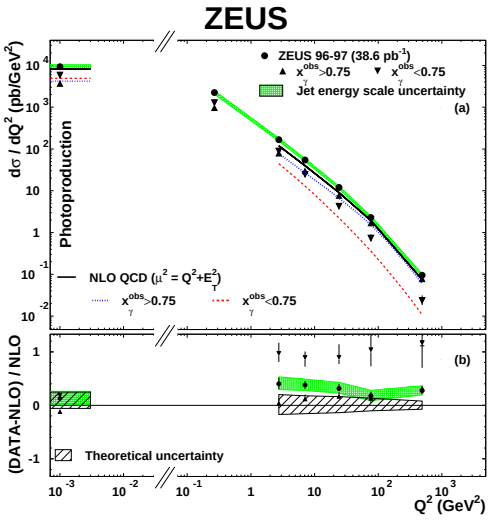

Figure 6. ZEUS dijet cross-section as a function of Q^2. Separately shown are the direct- and resolved-enriched samples and their description by the NLO QCD calculation.

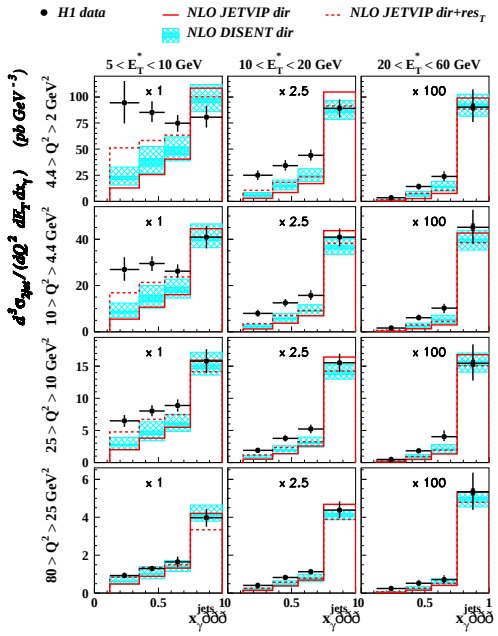

Figure 7. H1 triple-differential dijet cross-section.

Q^2 region. However, the prediction is very sensitive to the renormalisation scale choice, and scale choices can be made such that the data are compatible with the predictions. For the photoproduction region, which also is dominated by low x_γ values, the (direct+resolved) NLO calculation is able to describe the data.

H1 has measured the triple-differential dijet cross-section $d^3\sigma/d\overline{E}_T dQ^2 dx_\gamma$ [7] ($\overline{E}_T$ is the mean transverse energy of the two jets). Also here the conclusion is that at low Q^2 and also at low values of $\overline{E}_T$ NLO QCD calculations fail to describe the data at low values of x_γ. This is the case even if the calculations include the contributions from the resolved photon (Figure 7). In the same analysis, H1 could also demonstrate the importance of the initial and final state parton showers which help considerably in describing the data with LO MC models.

4.5. PARTON DYNAMICS AT LOW x

Another problematic issue in jet physics is the question of parton dynamics at low x. Earlier studies of so-called forward jets [8] were designed to hunt for the break-down of DGLAP evolution and the onset of BFKL signatures. However, the results were never really conclusive, mainly because no NNLO DGLAP calculation and no BFKL prediction usable for experimentalists were (and are) available. Also the influence of resolved contributions to the predictions was unclear.

There are new results by the H1 collaboration on forward jet and π^0 production in low Q^2 DIS [9,10]. The forward jet analysis, which was performed in the kinematic region $5 < Q^2 < 85$ GeV^2, studied the triple-differential cross-section $d^3\sigma/d\overline{p}_T^2 dQ^2 dx$ and compared the data to NLO QCD calculations and various MC models [9]. One result is shown in Figure 8, where the data are presented as a function of x and are compared to the NLO QCD calculation which clearly fails to describe the data at low values of x. MC models implementing resolved photon contributions and models using the the colour-dipole model come close to the data, although

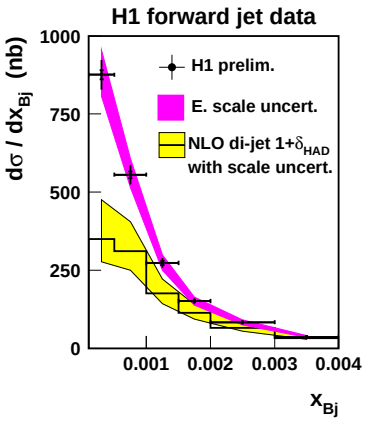

Figure 8. H1 forward jet measurement as a function of x. The data are compared to (direct) NLO QCD calculations. Also indicated are the energy scale and renormalisation scale uncertainties.

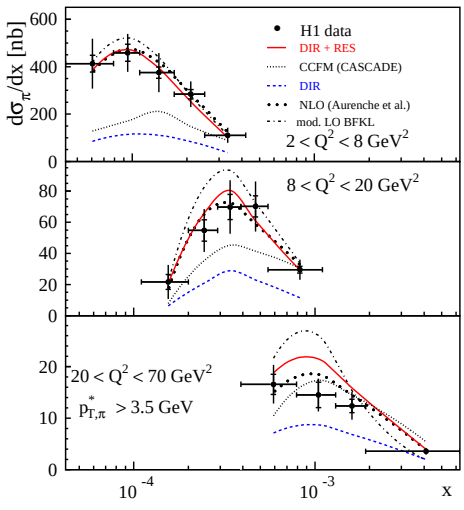

Figure 9. H1 forward pion measurement as a function of x. The data are compared to various QCD calculations and models.

a discrepancy between data and predictions remains at lowest values of x. A more differential study shows that the discrepancies are largest for low transverse energies and low Q^2.

For the case of forward π^0 production [10], most of the available predictions do a sufficiently good job. Figure 9 shows the forward π^0 cross-section as a function of x in three bins of Q^2; the good description of the data by most models (including the NLO calculation involving a convolution of matrix elements and fragmentation functions) is prominent.

5. STRANGE PENTAQUARKS

The measurement of narrow baryonic resonances of positive strangeness in the K^+n and K^0_Sp decay channels with a mass of about 1530 MeV and a very narrow width has recently raised a lot of attention. The findings are consistent with five-quark bound states, so-called pentaquarks, $\Theta^+ = uudd\overline{s}$.

The ZEUS collaboration started a search for the strange (anti)pentaquark in the $K^0_Sp(\overline{p})$ channel [11], relying mainly on the precise tracking information from the central drift chamber. The analysis used all events with $Q^2 > 1$ GeV^2 of the full 1996-2000 data statistics of 121 pb^{-1}, about 1.600.000 events.

The $K^0_Sp(\overline{p})$ invariant mass was obtained by combining the K^0_S and (anti)proton candidates and fixing the kaon mass to the PDG value. Figure 10 shows the resulting pentaquark candidate mass distribution together with the fit (a background function and two gaussians), the background function and the prediction of the ARIADNE Monte Carlo. A clear peak at 1522 MeV with a width of about 6 MeV is visible. The number of events ascribed to the signal is 221±48, of which 96±34 are in the antiproton channel. Thus, not only could the pentaquark be confirmed, but also the first observation of the antipentaquark with quark content $\overline{uudd}s$ was made.

The charmed pentaquark state that was observed by the H1 collaboration will be discussed in another proceedings contribution [12].

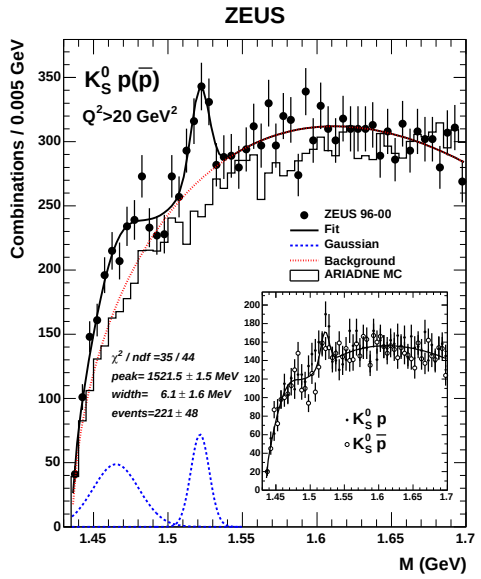

Figure 10. The ZEUS pK^0_S ($\overline{p}K^0_S$) invariant mass distribution with the peak at about 1522 MeV. Also shown are the results of a fit with a background function and two gaussians, the background function and the simulation of the ARIADNE Monte Carlo.

6. OTHER SELECTED TOPICS

6.1. QCD instantons

Instantons are non-perturbative fluctuations of the gauge fields in non-abelian gauge theories. But although instantons are predicted by the standard model, they have not been observed so far. Especially QCD instantons, however, are supposed to have short-distance implications at sufficiently low energies; they are, for example, supposed to induce characteristic topologies in DIS ep scattering events. Results on instanton searches have been reported on by the H1 collaboration before [13]. Recently the ZEUS collaboration has published the results of a search for instanton events [14] performed in about 40 pb^{-1} of data collected in the years 1996/97. The data were selected according to $Q^2 > 120$ GeV^2. For the search for instanton events, several discriminating techniques were applied which distinguish between standard NC DIS events and instanton events using multi-dimensional cuts. Instanton events were simulated using the QCDINS calculation which predicts an instanton cross-section of 8.9 pb. Under the assumption that all selected data events are instanton events, an upper limit on the instanton production cross-section of $\sigma < 26$ pb was derived at 95 % C.L.

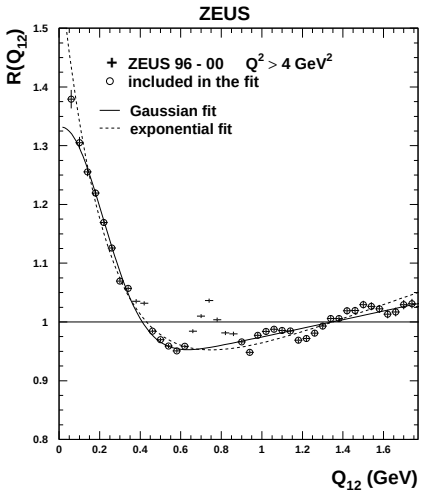

Figure 11. Bose-Einstein correlations: ZEUS measurement of $R(Q_{12})$ for $Q^2 > 4$ GeV^2 together with two fits. The data points included in the fit are marked with circles.

6.2. Bose-Einstein correlations

ZEUS has measured Bose-Einstein (BE) correlations in NC DIS over a wide kinematic range in Q^2 from 0.1 GeV^2 to 8000 GeV^2 [15] in over 120 pb^{-1} of data collected from 1996 to 2000. As a measure for the correlation, the analysis used the double ratio $R(Q_{12}) = \zeta^{data}/\zeta^{MC,noBE}$, where Q_{12} is the Lorentz-invariant momentum difference of the particles (which are assumed to be pions), and ζ^{data} ($\zeta^{MC,noBE}$) are the ratios of inclusive two-particle densities for like-sign and unlike-sign bosons, $\zeta = \rho(++,--)/\rho(+-)$, for data and Monte Carlo, respectively. The Monte Carlo sample was generated without simulating

Bose-Einstein effects, assuming that BE correlations can be factorised from other types of correlations and that non-BE correlations are well described by the MC models. Therefore $R(Q_{12})$ should be sensitive to BC correlations only.

Figure 11 shows the double ratio $R(Q_{12})$ together with two fit models which aim at extracting the size r of the source of final state pions and the coherence parameter λ. The data points marked with circles were actually included in the fit; as expected the parameters extracted from the gaussian fit show no dependence on Q^2. The radius of the production volume is found to be about $r \sim 0.65$ fm, and the coherence parameter $\lambda \sim 0.47$. A two-dimensional study of the Bose-Einstein effect shows that the pion-emitting region is elongated. All findings are compatible with measurements from other experiments and colliders.

6.3. Anti-Deuteron production

The H1 collaboration has measured anti-deuteron production [16] and compared the production rate to results from central proton-proton (Au-Au) collisions measured at the CERN ISR (RHIC).

No significant signal can be found for positively charged tracks, but for negatively charged particles a clear signal of 45 anti-deuterons with an estimated background of about 1 event is observed, leading to a total anti-deuteron cross-section of about 2.7 nb.

The production of nuclei in particle collisions can be described in terms of the coalescence model in which the cross-section σ_A for the production of a nucleus with A nucleons can be related to the cross-section for the production of free nucleons in the same reaction, σ_N, by a so-called coalescence parameter B_A.

The (anti-)deuteron coalescence parameter value $B_2 \sim 0.01$ found by ZEUS is compatible with values deduced at lower center-of-mass energies in pp and pA collisions, but much larger than observed in $Au - Au$ collisions at similar nucleon-nucleon center-of-mass energies. This is understandable if the size of the hard reaction 'fireball' is much smaller in pp / γp than in heavy ion collisions.

7. CONCLUSION

Jet and hadronic final state physics at HERA has been reviewed. Clear progress especially in jet physics in terms of statistical precision has been made over the past few years. Jets have even been used in global QCD fits with the aim of improving the knowledge of the gluon density at high values of x. In addition, exotic signatures like instantons or pentaquarks have been analysed. Nevertheless, HERA physicists are eagerly waiting for HERA 2 data which promise enough statistics to solve remaining questions and to come to firmer conclusions concerning α_S and the PDFs.

ACKNOWLEDGEMENT

I would like to thank my colleagues from H1 and ZEUS for their support and the conference organisers for a pleasant stay in Montpellier.

REFERENCES

1. ZEUS Coll., Abstract 5-0290, ICHEP 2004.
2. ZEUS Coll., DESY-04-016.
3. ZEUS Coll., DESY-04-072.
4. ZEUS Coll., Abstract 5-0263, ICHEP 2004.
5. H1 Coll., DESY-03-160.
6. ZEUS Coll., DESY-04-053.
7. H1 Coll., DESY-03-206.
8. H1 Coll., Nucl. Phys. B538 (1999) 3;
   ZEUS Coll., Phys. Lett. B474 (2000) 1,233;
   ZEUS Coll., Eur. Phys. J. C6 (1999) 239.
9. H1 Coll., H1prelim-04-033.
10. H1 Coll., DESY-04-51.
11. ZEUS Coll., DESY-04-164.
12. K. Lipka, these proceedings.
13. H1 Coll., Eur. Phys. J. C25 (2002) 495.
14. ZEUS Coll., DESY-03-201.
15. ZEUS Coll., DESY-03-176.
16. H1 Coll., DESY-04-032.